



HAL
open science

Single-step electrohydrodynamic separation of 1–150 kbp in less than 5 min using homogeneous glass/adhesive/glass microchips

Bayan Chami, Nicolas Milon, Juan-Luis Fuentes Rojas, Samuel Charlot, Jean-Christophe Marrot, Aurélien Bancaud

► **To cite this version:**

Bayan Chami, Nicolas Milon, Juan-Luis Fuentes Rojas, Samuel Charlot, Jean-Christophe Marrot, et al.. Single-step electrohydrodynamic separation of 1–150 kbp in less than 5 min using homogeneous glass/adhesive/glass microchips. *Talanta*, 2020, 217, pp.121013. 10.1016/j.talanta.2020.121013 . hal-03024740

HAL Id: hal-03024740

<https://laas.hal.science/hal-03024740>

Submitted on 9 Dec 2020

HAL is a multi-disciplinary open access archive for the deposit and dissemination of scientific research documents, whether they are published or not. The documents may come from teaching and research institutions in France or abroad, or from public or private research centers.

L'archive ouverte pluridisciplinaire **HAL**, est destinée au dépôt et à la diffusion de documents scientifiques de niveau recherche, publiés ou non, émanant des établissements d'enseignement et de recherche français ou étrangers, des laboratoires publics ou privés.

Single-step electrohydrodynamic separation of 1-150 kbp in less than 5 min using homogeneous Glass/Adhesive/Glass microchips

Bayan Chami¹, Nicolas Milon^{1,2*}, Juan-Luis Fuentes Rojas^{1*}, Samuel Charlot^{1*}, Jean-Christophe Marot¹, Aurélien Bancaud¹

AFFILIATION

¹CNRS, LAAS, 7 avenue du colonel Roche, F-31400, Toulouse, France.

²Adelis Technologies, 478 Rue de la Découverte, 31670 Labège, France

**These authors have equally contributed to the work*

ABSTRACT (198 words)

Electrohydrodynamic migration, which is based on hydrodynamic actuation with an opposing electrophoretic force, enables the separation of DNA molecules of 3 to 100 kbp in capillary systems within one hour. Here, we wish to enhance these performances using microchip technologies. This study starts with the development of a fabrication process to obtain microchips with uniform surfaces, which is motivated by our observation that band splitting occurs in microchannels made out of heterogeneous materials such as glass and silicon. The resulting glass-adhesive-glass microchips feature the highest reported bonding strength of 11 MPa for such materials (115 kgf/cm²), a high lateral resolution of critical dimension 5 μm, and minimal auto-fluorescence. These devices enable us to report the separation of 13 DNA bands in the size range of 1-150 kbp in one experiment of 5 minutes, i.e. 13 times faster than with capillary electrophoresis. In turn, we provide evidence that band splitting in heterogeneous glass-silicon microchips arises from differential Electro-Osmotic Flow (EOF) in between the upper and lower walls of the channel. We further indicate that differential EOF occurs in microchip electrophoresis and constitutes an underappreciated source of band broadening. We finally prove that our separation data compare favorably to state-of-the-art microchip technologies in terms of resolution length and theoretical plate numbers.

INTRODUCTION

The gold standard in genetic analysis is capillary electrophoresis, which is based on the migration of DNA molecules through a separation matrix that slows them down proportionally to their molecular weight (MW) (Viovy 2000). Using a continuous and mono-directional electric field, separation performances reach a limit above a threshold size on the order of ~ 10 kbp (Viovy 2000; Dorfman 2010). The use of pulsed-field increases this size threshold by up to two orders of magnitude, however at the expense of overly long separation times of 10 hours (Dorfman 2010). Alternatively, free solution DNA separation based on hydrodynamic actuation in narrow capillaries of ~ 2 μm enabled the fractionation of molecules of up to 100 kbp in one hour (Wang et al. 2012). The combination of electrophoresis and hydrodynamics acting in opposite directions, hereafter called electrohydrodynamic migration, also appeared as a free solution separation technology efficient for long molecules, as initially reported with 5 and 50 kbp DNA (Zheng and Yeung 2002) and recently improved in the range of 3 to 200 kbp with a separation time of one hour (Milon et al. 2019). In order to consolidate the promising performances of electrohydrodynamic migration, which relies on the existence of size-dependent transverse forces that set molecules close to the walls (Ranchon et al. 2016) (ADD here 2 papers from Butler), we wished to test whether microchips would allow us to gain time and extend the separation range.

DNA separation techniques have indeed benefited from microchip technologies in reducing sample consumption and analysis time and increasing the sensitivity and efficiency (Pfohl et al. 2003). Gains in performance have been achieved through the control of sample injection using sophisticated channel geometries (Nathan A. Lacher et al. 2001), as well as the engineering of artificial matrices tailored for low or high MW molecules (Doyle et al. 2002; Kaji et al. 2004; Rahong et al. 2014; Cao and Yobas 2014). The fabrication of microchips relies on the assembly of a patterned substrate with a transparent one using a variety of micromachining and bonding technologies. The transparent substrate is most often made out of glass, which remains the most relevant material for analytical microfluidics due to its chemical, mechanical and electric resistance in addition to its transparency and low background fluorescence, which make it ideal for optical detection (Giri 2017). In contrast to capillaries, which present homogeneous surfaces, microchip devices are in general heterogeneous in composition, for instance with polymer/glass or silicon/glass walls. Yet, some reports have shown the degradation of separation performances in microchips made out of hybrid materials (M.-S. Kim et al. 2005). We therefore set out to perform our experiments in conventional silicon-glass microchips as well as in specifically developed microfluidic devices with homogeneous surfaces.

The first section of this paper presents the fabrication process of selectively bonded glass-glass microchips with an epoxy-based negative resist (PermiNex). The characterization of these microchips notably shows the highest bonding strength of ~ 11 MPa (115 kg/cm^2), enabling the application of pressures up to 7 bar during separation experiments. We then probe the migration of high MW molecules using electrohydrodynamics in homogeneous PermiNex-bonded *vs.* heterogeneous microchips obtained by silicon-glass anodic bonding. DNA bands tend to split in heterogeneous chips, but remain stable in Perminex-bonded devices. We propose that this effect

stems from the difference in electroosmotic flow (EOF) in between the upper and lower walls of slit-like microchannels. By investigating DNA electrophoretic transport, we further suggest that differential EOF accounts for the build-up in band broadening in heterogeneous chips. Finally, we perform a long-range separation of 13 DNA bands from 1 to 150 kbp in PerminNex bonded glass-glass microchips, which is achieved in less than five minutes with a resolution length (minimum resolvable size) and theoretical plate number that compare well to the state of the art microchip techniques. Altogether, we conclude that DNA electrohydrodynamic separation performances can be enhanced using microchips fabricated with the Perminex bonding technology.

MATERIALS AND METHODS

We used four-inch wafers of 500 μm thick alkali-free glass AF 32® (Schott) and p-doped silicon wafers. silicon/glass chips were fabricated following the process described in ref. (Ranchon et al. 2016). Photoresists were purchased from Microchem Corp. Cleaning steps were carried out with oxygen plasma (TEPLA) at a power of 400 W and a flow rate of 1000 ml/min for 5 min. We performed tests of adhesion using XYZTEC Condor Sigma bond tester with chips of 0.25 cm^2 .

Experimental setup:

Polymer solution PVP (polyvinylpyrrolidone) 10 KDa 2.5% (w/v) (Sigma Aldrich) is prepared in TBE 1X (Tris-Borate-EDTA) (Sigma Aldrich) and supplemented with 2% (w/v) DTT (Dithiothréitol, Sigma Aldrich). The solution is then filtered with 0.2 μm pore syringe filter. 150 kbp BAC-clone DNA band (gift from CNRGV) or phiX174 DNA (5,386 bp, Sigma Aldrich) are diluted in a volume of the PVP solution at a concentration of 0.3 μM . Intercalating dye YOYO-1 (Thermo Fischer) is used to label the DNA at a ratio of 1:8 (1 intercalating molecule per 8 base pairs).

Microfluidic channels in Si/glass and glass/glass are filled with 70% ethanol to eliminate bubbles. The channels are then filled with PVP buffer followed by an injection, at the inlet, of PVP containing the labeled DNA molecules. A pressure and voltage are applied across the T-shaped channels to create opposing hydrodynamic and electrophoretic flows. Lateral flows are applied from the side channels to concentrate the DNA in a plug that is then pushed into the main separation channel where the DNA bands are detected by an sCMOS camera (Andor Zyla) at 35 mm from the T-junction (see Fig. 2 in Results). Fluorescence intensity as a function of time is recorded and peaks are fitted using Igor Pro (WaveMetrics).

Metrics of the separations:

We compared the separation of 1-150 kbp DNA ladder to those of state of the art microchip technologies using two parameters; the resolution length (RSL) and the theoretical plate number. The RSL in bp defines the smallest size that can be resolved and is given by:

$$RSL = \frac{\Delta n}{R_s} \quad (1)$$

where Δn is the difference in base pair between consecutive bands, and R_s the resolution obtained at baseline by fitting the peaks with a Gaussian distribution. For temporal separations, the resolution is calculated as follows:

$$R_s = \frac{2(t_2 - t_1)}{w_1 + w_2} \quad (2)$$

where t is the migration time of the DNA band and w the width of the band at the baseline. For spatial separations, we similarly define $R_s = \frac{2(x_2 - x_1)}{w_1 + w_2}$, where x is the spatial position of the band.

The theoretical plate number (N) is a measure of the separation efficiency, which is calculated for separations in time, using the following formula:

$$N = 16 \left(\frac{t}{w} \right)^2 \quad (3)$$

where t is the migration time of the band and w is its baseline width. To perform the comparison between different separation techniques, theoretical plate number per meter is used instead. It is defined as:

$$\textit{Theoretical plate number per meter} = \left(\frac{N}{L} \right) \times 100 \quad (3)$$

Where L is the separation length in cm.

RESULTS

Fabrication of homogeneous glass microchips with high-resolution:

Two approaches can be considered to fabricate homogeneous glass microfluidic devices, namely (i) the formation of channels by photolithography and etching followed by glass-to-glass bonding, or (ii) selective bonding using photo-patternable adhesives or glass frit. The former approach is mostly carried out with fusion bonding (Stjernström and Roeraade 1998), which amounts to fusing glass substrates together under pressure and temperature of up to 600° C (Deng 2015). Similar techniques include plasma activated bonding (Howlader, Suehara, and Suga 2006; Y. Xu et al. 2012) and UV bonding (Schlautmann et al. 2003), yet they require immense care for the cleanliness of the glass substrates (Mayer, Marianov, and Inglis 2018). On the other hand, glass frit bonding, which involves the use of an intermediate glass frit layer heated until molten enabling the hermetic sealing of wafers (Knechtel 2015), suffers from its low lateral resolution, which makes it difficult to define straight channel borders (Knechtel 2012).

We chose to perform selective bonding with a photo-patternable adhesive to circumvent most of these limitations.

The fabrication of PermiNex microchips starts with the spin coating of a positive resist AZ ECI 3027 and exposure to UV through a negative polarity mask of a glass wafer (Fig. 1a-b). Two layers of amorphous silicon (a-Si) of 120 nm and SiO₂ of 200 nm are deposited by inductively coupled plasma enhanced chemical vapor deposition (PECVD) (Fig. 1c). The wafer is cleaned and 3.5 mL of the adhesive photoresist PermiNex® 2005 is spin-coated to form a 2.5 μm film (Fig. 1d-e). The soft bake is performed at 95 °C during 9 min followed by UV exposure for 45 sec at 870 mJ/cm² using the same negative polarity mask, in hard contact and with alignment with the a-Si/SiO₂ patterned layer (Fig. 1f). The post-exposure bake time is set to 6 min at a temperature of 72 °C. Note that this step is critical for the conservation of the patterns during the development with the organic SU8-developer during one min. The final step is a hard bake at 180 °C for 5 min. The wafer is then cleaned using O₂ Plasma for 2 min at low power and flow rate of (200 W and 400 mL/min), enough to remove organic contaminants but at the same time preserve the adhesive resist. A decrease in the adhesive thickness of 300 +/- 100 nm is noticed after the Plasma treatment. The wafer is eventually clamped with another glass wafer, where via holes are drilled by sand blasting, using the fixture of Bond Aligner (Suss MicroTec) to perform the alignment (Fig. 1g). The temperature and pressure program consists of heating the wafers to 150-200 °C and applying a pressure of 4-5 bar for 30 sec establishing a force of 10-16 kN under vacuum (5×10⁻² mbar). The whole bonding process takes less than 15 min. An SEM image of the formed 2-μm channel is shown in supplementary Figure S1.

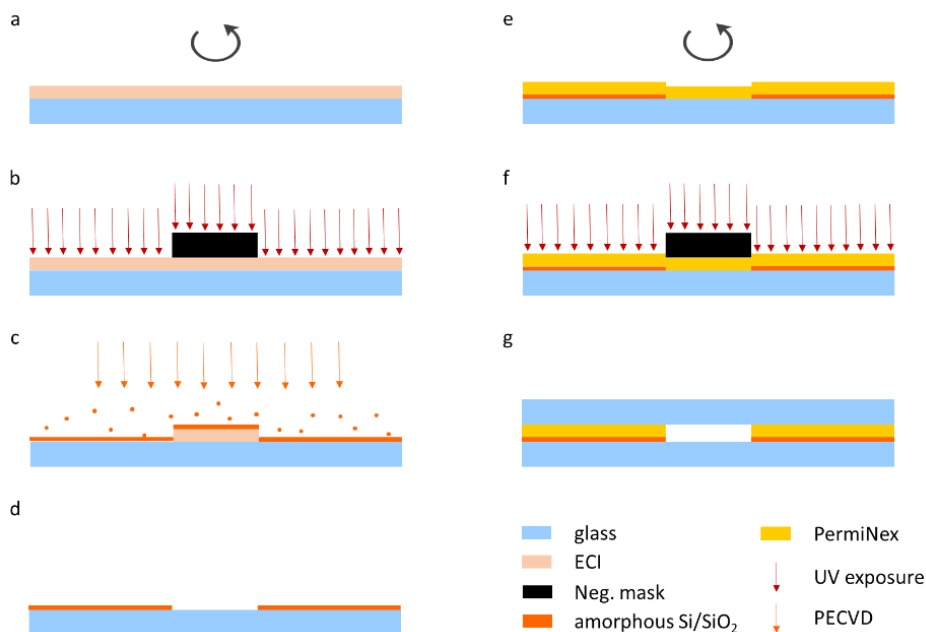


Figure 1: Glass/PermiNex/Glass process flow. (a) Spin coating of the positive photoresist AZ ECI 3027 on a glass wafer. (b) UV exposure with the use of a negative mask following the standard protocol. (c) a-Si and oxide deposition using PECVD. (d) ECI development using acetone. (e) Spin coating of PermiNex at a speed of 8000 rpm and acceleration of 2500 rpm/s for 60 sec. (f) UV exposure with a negative mask and development of PermiNex with SU-8 developer. (g) Adhesive bonding of the two glass wafers with PermiNex as intermediate layer.

Using a microchip design with a funnel-shape geometry, as reported in (Chami et al. 2018), we demonstrate the ability to fabricate channels with critical size of 5 μm using a layer of PermiNex of 2.2 \pm 0.1 μm by comparing the mask feature to that imprinted in the final microchip (Fig. 2a). Since the process comprises a low temperature bonding step, gold electrodes of 200 nm in thickness can be fabricated on the glass substrate and glued with the PermiNex layer (Fig. 2c-d). The PermiNex layer adheres very well to the gold and no leakage is observed at the level of the electrodes or any other area in the device (data not shown). This integration scheme can serve to perform electrical operation, such as electrochemical and/or amperometric detection.

Tests of adhesion with pull-off tensile machine (see Methods) show that the bond fracture failed each time because of either die fracture or breaking of the glue attaching the dolly to the chips. Using shear tests, we evaluate the bonding strength of ~ 11 MPa (115 kgf/cm²) before the glass breaks. It is the highest bonding strength, to our knowledge, obtained for glass/adhesive/glass microchannels in comparison to SU-8 (S G Serra et al. 2007), BCB (Niklaus 2002), and silicone-based resins (J. Kim et al. 2012). The PermiNex bonding breaks with a maximum pull force of 2.93 kgf bonding (~ 1.15 MPa bond strength) only when the microchips is heated at 50°C. At this stage, the bonding is irreversible unlike in processes that use wax as bonding adhesive (Gong et al. 2010).

The final microchips offer several advantages for electrohydrodynamic separation. First, the bonding strength enables the application of pressures of up to 7 bar for separation experiments. Second, the PermiNex microchips withstand very high electric fields, whereas breakdown of the oxide layer occurs for a maximum applied voltage of 450 V using an oxide layer of 400 nm in anodically bonded silicon/glass chips (Supplementary Fig. S2). Specifically, we did not detect any problems as we used electrophoretic actuation with up to 800 V, *i.e.* with electric fields of more than 200 V/cm (not shown).

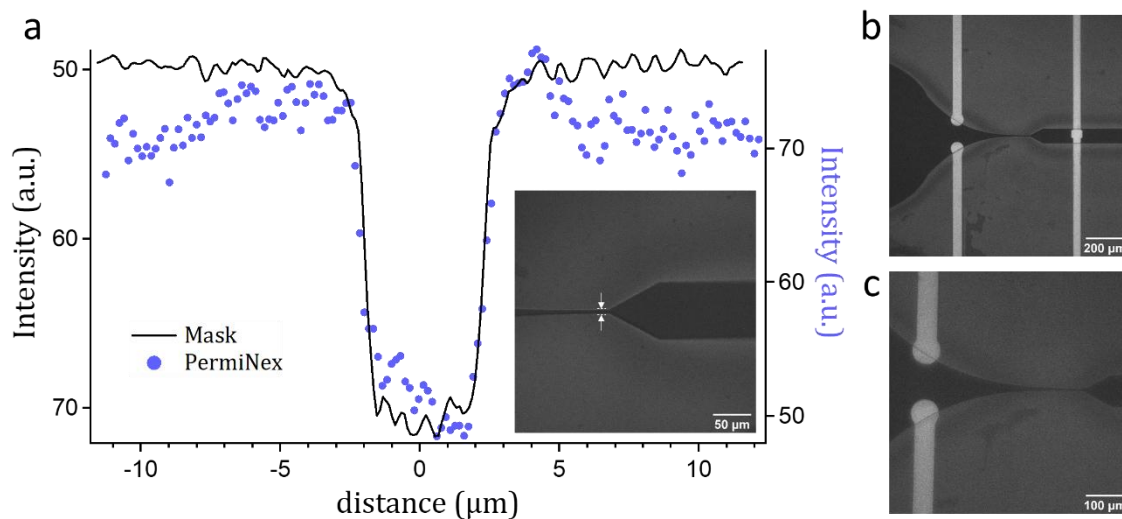


Figure 2: High-resolution microfluidic funnel geometries and electrode integration. (a) Comparison between the chromium mask feature of 5 μm critical size and the microfluidic funnel geometry patterned using PermiNex (shown in inset). (b) and (c) present bright field images of the microchip with integrated 200 nm gold electrodes.

Minimization of PermiNex auto-fluorescence:

One disadvantage of PermiNex comes from its high auto-fluorescence in the entire visible spectrum (Kubicki, Walczak, and Dziuban 2016). A patterned a-Si layer, which is strongly adsorbing light in the visible spectrum, is deposited underneath the PermiNex layer (Fig. 1) in order to block the excitation and emission light and hence reduce auto-fluorescence. Figure 3 shows a glass/glass chip bonded directly with PermiNex without the deposition of a-Si (panels a & c) versus a chip where an a-Si layer of 120 nm and an oxide layer of 200 nm are deposited before the spin-coating of PermiNex (panels b & d). A slight miss-alignment between the PermiNex layer and the a-Si layer allows seeing the channel borders in Fig. 3b. As an example of the adverse effects of PermiNex auto-fluorescence, we report fluorescence micrographs of 150 kbp DNA molecules in the course of their electrophoretic migration in a separation microchip (Fig. 3 c & d, design of the chip in Fig. 3e). Even with the use of a field diaphragm to mask the autofluorescence signal from the PermiNex layer, the signal to noise ratio of individual molecules increases by a factor of 1.35 with the absorbing layer (dark blue curve in Fig. 3f). Consequently, our microchip fabrication process is readily suited to bioanalytical operations with a minimal signal to noise ratio and a strong resistance to pressure and electric fields.

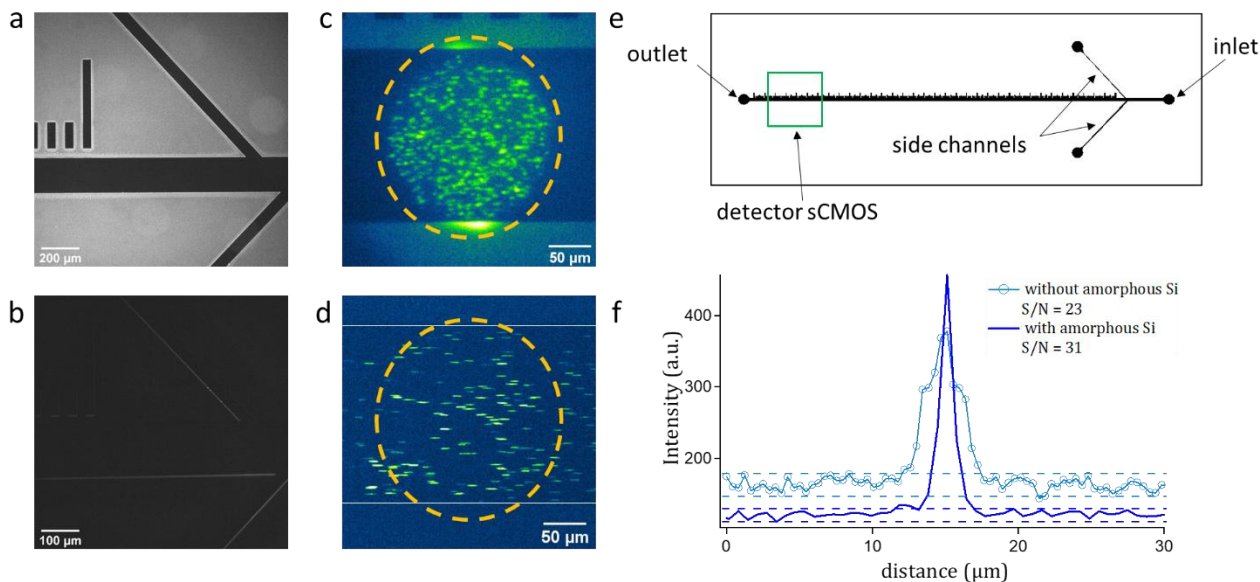


Figure 3: Blocking the auto-fluorescence of PermiNex. . (a) Glass/glass chip bonded using PermiNex without the deposition of an a-Si layer. (b) Glass/glass bonded chip with an a-Si and oxide layers deposited below the PermiNex layer. The auto-fluorescence is totally blocked. A slight misalignment between the PermiNex and a-Si layer allows distinguishing the channel borders. (c) and (d) A plug of DNA migrates in channels without and with a-Si layer, respectively. (e) The design of a 4 cm microchip where a plug of DNA is formed at the junction with side channels and the fluorescence detector placed 35 mm away. (f) The S/N ratio is calculated for molecules in (c) and (d), it increases by a factor of 1.35 with the blocking layer.

Peak splitting in silicon/glass microchips is suppressed in glass/PermiNex/glass microchips:

We then focus on DNA electrohydrodynamic migration in Glass-glass vs. heterogeneous microchips. We perform experiments with a single DNA band of 150 kbp and electrohydrodynamic actuation associated to maximum flow and electrophoretic velocities of $V_0 = 0.5 \text{ mm/s}$ and $V_E = 0.11 \text{ mm/s}$, respectively. In glass/Si microchips, we notice that the DNA band splits into two populations of equal intensity in front of the detector placed 35 mm downstream of the injection plug (see chip design in Fig. 3e, Cyan curve in Fig. 4c). The analysis of the fluorescence micrographs recorded by the camera indicates that the two DNA bands migrate at different vertical positions across the channel height. A first DNA “band” appears to be out of focus (close to the Si wall) at $t=30.6 \text{ s}$ (Fig. 4a) and the second one in focus (close to the glass wall) at $t=39 \text{ s}$ (Fig. 4b). Small white arrows pointing contaminations stuck to the glass wall help indicate the difference in focus between the two DNA populations.

Splitting can readily be eliminated in PermiNex-bonded microchips using the same actuation settings (dark blue curve in Fig. 4c). It can also be recovered in “asymmetric” PermiNex microchips (intermediate blue curve in Fig. 4c) obtained with the same fabrication protocol except that PermiNex is developed with its standard developer that contains the quaternary ammonium salt Tetramethylammonium hydroxide (TMAH). Because TMAH is known to etch SiO_2 surfaces (Chen et al. 2001; Biswas and Kal 2006; Suttijalern, Prabket, and Niemcharoen 2018), the development step likely creates differential roughness in between the two glass surfaces, *i.e.* heterogeneities in surface properties despite the the same composition. Consequently, differences in surface molecular composition or in roughness appear to trigger splitting in electrohydrodynamic separation.

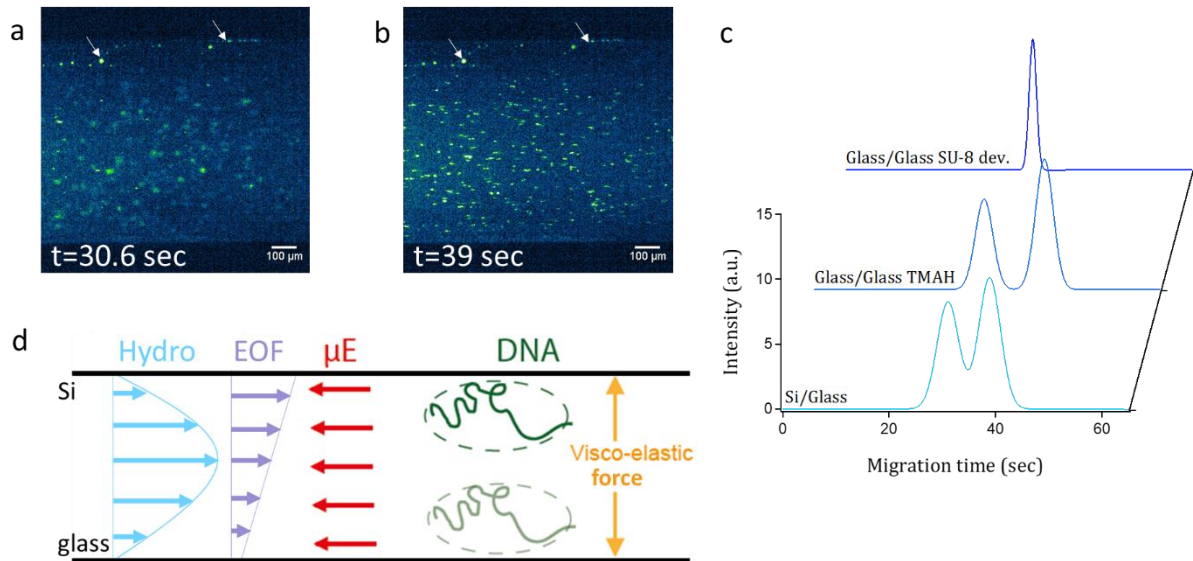


Figure 4: Evidence of band splitting in Silicon/Glass chips. (a) Time sequence of a 150 kbp DNA band in a Si/glass channel at the detecting region showing unfocused DNA molecules migrating close to the Si surface after migration time of 30.6 sec and (b) focused DNA molecules migrating close to the glass surface and passing in front of the detector 8.4 sec later. The small white arrows point small contaminations stuck to the glass surface, which demonstrate the difference in focus between the two DNA populations. (c) Fluorescence intensity profiles showing a

150 kbp DNA band broadening and splitting into two bands in Si/glass and glass/glass chips developed with TMAH versus a unique band in glass/glass chips developed with SU-8 developer (organic solvent). (d) Diagram illustrating the viscoelastic migration of DNA molecules to the channel walls in opposing electrohydrodynamic flows. The difference between the Si and glass surfaces electrochemical properties induces heterogeneity in the EOF close to the two surfaces.

We suggest that peak splitting stems from the difference in EOF between the upper and lower surfaces of the microchip. Differential EOF indeed induces a shear Couette-like flow across the channel height (purple arrows in Fig. 4d) (Andreev, Dubrovsky, and Stepanov 1997a). Because transverse migration to the walls is dictated by the fluid viscoelastic properties (Chami et al. 2018), we suggest that molecules travel at the same distance from the upper and lower wall, *i.e.* at equal hydrodynamic velocities, and that the peak splitting is dictated by the difference of EOF.

Notably, the consequences of differential EOF readily appear in electrohydrodynamic transport, because DNA spatial distribution is uneven across the channel height. Should this effect occur in electrophoresis, we expect the shear flow induced by differential EOF to create mixing by some type of Taylor dispersion mechanism arising from the coupling of longitudinal speed gradients with transverse diffusion. Accordingly, previous electrophoresis studies have shown that even a 10% difference in the zeta-potential between upper and lower walls of a microchip leads to band broadening (Andreev, Dubrovsky, and Stepanov 1997b; Bianchi et al. 2001; Herr et al. 2000). We set out to check our proposition further by performing another set of experiments with electrophoresis only.

Evidence for differential electro-osmosis in Si/glass microchips:

Using silicon-glass chips, we probe the response of single phiX-174 DNA with three values of the electric field. Note that phiX-174 only contains 5 kbp MW, but its spherical shape under the microscope simplifies its tracking. The trajectories of 40 molecules, each containing 100 points at least, have been recorded in 2D in order to extract the velocity distribution along and across the electric field direction as was performed by our team to characterize confined flows (Ranchon, Picot, and Bancaud 2015). The lateral velocity distribution (perpendicular to electrophoresis direction), centered at zero, represents Gaussian noise due to thermal diffusion (green histogram in Fig. 5a). The longitudinal velocity distribution (along the electrophoresis direction) is instead shifted due to electrophoretic advection (blue histogram in Fig. 5a). Assuming the electrophoretic force to be homogeneous across the channel height, we expect the longitudinal dispersion to equate that in the transverse direction. However, we notice that the breadth in the longitudinal *vs.* lateral direction is increased by a factor of 1.2, consistent with the observation that the diffusion coefficient characterizing DNA bands in electrophoresis is larger than that expected from Brownian fluctuations (Ross, Johnson, and Locascio 2001). Furthermore, this onset appears to increase with the amplitude of the electric field by a factor of 1.1 to 1.7 for an electrophoretic velocity of 9.8 and 21 $\mu\text{m/s}$, respectively (not shown).

We then test whether the increase of the breadth stems from a difference in EOF between the upper and lower channel walls. Considering that a molecule travels at V_{elec} by electrophoresis, the effect of the electroosmotic mobility V_{eof} , assumed to be homogeneous at the upper and lower wall, sets the DNA net velocity to $V_{\text{elec}} - V_{\text{eof}}$ (Viovy 2000). In hybrid microchips, V_{DNA} then takes the form of an affine function (Andreev, Dubrovsky, and Stepanov 1997b):

$$V_{\text{DNA}}(z) = V_{\text{elec}} - \frac{z}{h} \{V_{\text{eof}}^{\text{up}} - V_{\text{eof}}^{\text{down}}\} - V_{\text{eof}}^{\text{down}} \quad (4)$$

Because molecules can be assumed to be evenly dispersed in z , the longitudinal velocity distribution is the deconvolution of a Heavyside function centered at $V_{\text{elec}} - (V_{\text{eof}}^{\text{up}} + V_{\text{eof}}^{\text{down}})/2$ of breadth $(V_{\text{eof}}^{\text{up}} - V_{\text{eof}}^{\text{down}})/2$ with the Brownian noise measured by the transverse velocity distribution (Fig. 5b). According to this model, the fit of the velocity distribution informs us on the difference in EOF between the glass and Si walls. By setting the electric field to three different values, we observe that the difference in EOF increases linearly as DNA velocity increase, passing through zero without electrophoresis and with a proportionality factor of 0.43 (Fig. 5c).

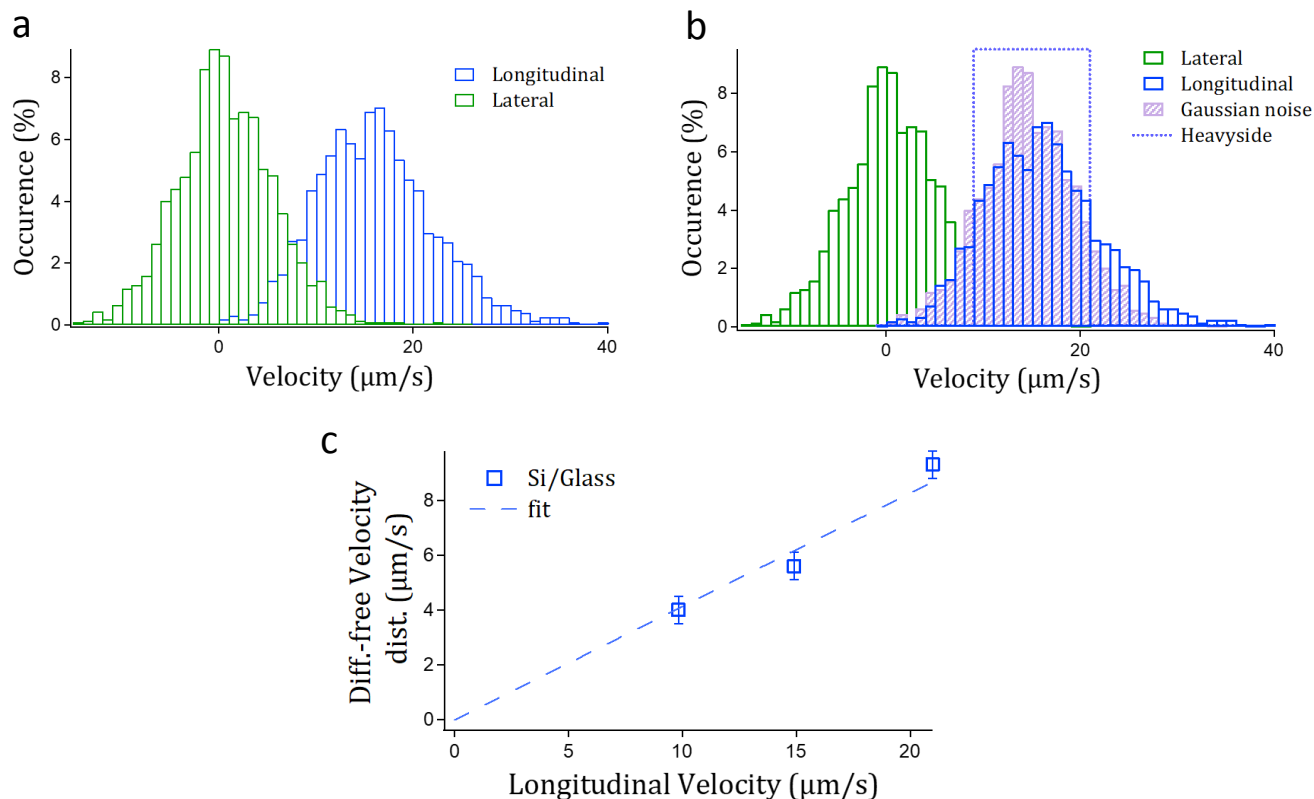


Figure 5: Analysis of DNA electrophoretic velocity distribution. (a) Velocity distributions of 2D tracked ϕX174 DNA molecules in a 2- μm Si/glass channel for a time interval of 100 ms. Lateral velocity distribution (green) representing thermal diffusion across the flow direction is centered at zero. Longitudinal velocity distribution (blue) is the convolution of Gaussian noise and diffusion-free velocity along the flow direction. (b) Analysis of the velocity distribution with a

Heavyside distribution. Using a Matlab code, the longitudinal velocity distribution is de-convolved to obtain the diffusion-free velocity distribution (represented by the Heavyside function) and the Gaussian noise. (c) Diffusion-free velocity distribution obtained in Si/glass channels. The difference in electroosmotic velocity expectedly increased linearly with the electric field, passing through zero without electrophoresis.

We then compare $V_{\text{eof}}^{\text{up}} - V_{\text{eof}}^{\text{down}}$ inferred from electrophoresis measurements to the difference of velocity between the two DNA peaks in electrohydrodynamic migration, shown in Fig. 4c. The time difference between the split DNA bands allows us to estimate that $(V_{\text{DNA}}^{\text{up}} - V_{\text{DNA}}^{\text{down}}) = 190 \mu\text{m/s}$. Furthermore, given that the electrophoretic velocity opposed to the hydrodynamic flow is equal to $460 \mu\text{m/s}$, we deduce that the ratio between the DNA split band velocity difference and the electrophoretic speed is 0.41. Hence, the broadening of the longitudinal velocity distribution observed with electrophoresis together with the splitting of DNA bands in electrohydrodynamic migration can be explained by the same difference in EOF in between the upper and lower walls of heterogeneous Si/glass chips.

Separation 1-150 kbp using a glass/PermiNex/glass T-shaped channel:

Finally, the newly fabricated glass/PermiNex/glass microchip is used for the separation of a kbp DNA ladder supplemented with a 150 kbp band, allowing us to cover more than two decades in MW from 0.5 kbp to 150 kbp. Optimal result is obtained by setting the pressure and voltage to 500 mbar and 170 V, respectively, corresponding to a flow speed of 0.6 mm/s and an electrophoretic velocity of $85 \mu\text{m/s}$. The separation of the 14 bands is achieved in less than 5 min (Fig. 6) with baseline separation for the bands from 2 kbp. The separation can be reproduced more than 10 times in the same chip without band splitting, demonstrating the relevance of our technology with homogeneous upper and lower surfaces. Consequently, the microchip format enhances the performances of electrohydrodynamic separations not only in terms separation time, which is decreased from 30 to 5 minutes, but also with a broader separation range starting from 1 instead of 3 kbp.

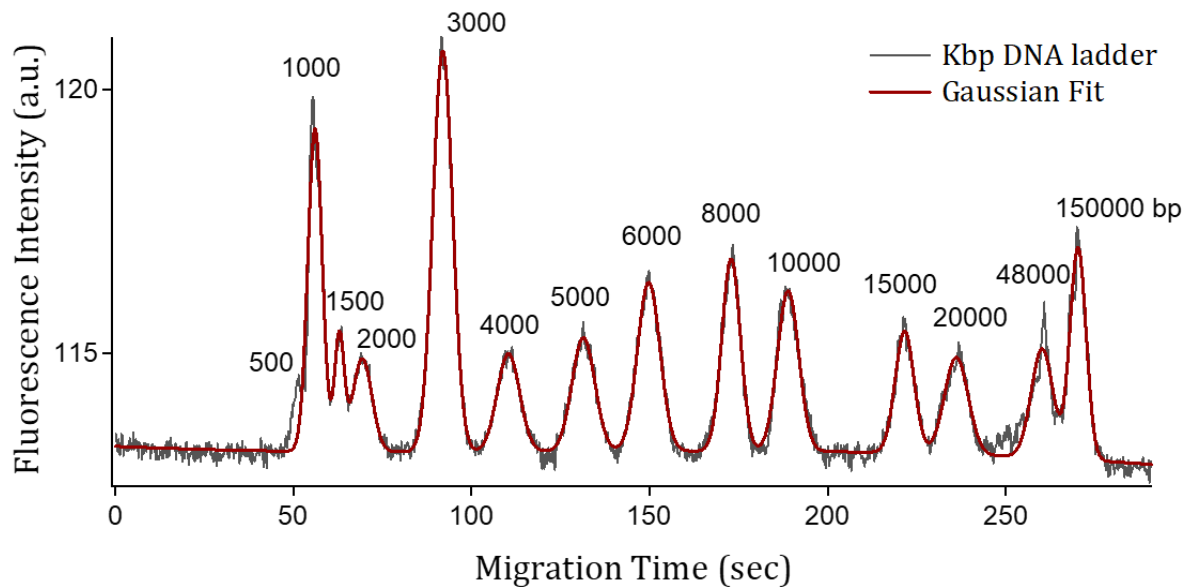


Figure 6: *Separation of 1-150 kbp DNA in a glass/PermiNex/glass channel. Fluorescence micrograph of a kbp DNA ladder separated in a glass/PermiNex/glass microfluidic chip using opposing electrohydrodynamic flows in viscoelastic polymer solution PVP 10 KDa 2.5%. The separation parameters are 500 mbar and 170 V, corresponding to a hydrodynamic speed of 0.6 mm/s and electric field of 42 V/cm, respectively.*

Comparison to microchip technologies for high MW DNA separation:

We now compare our separation performance to other microchip devices for fractionating high MW DNA (1-200 kbp). We use the resolution length (RSL) and theoretical plates per meter as readouts of the different techniques (see expression in the Method section) and report this data in plots (Fig. 7) as well as in Table 1.

Micro-capillary electrophoresis (MCE) devices with polymer matrices like linear polyacrylamide can be used for DNA separation in the size range of 1-10 kbp (Bousse, Dubrow, and Ulfelder 1998; Mueller et al. 2000; Lu and Liu 2006) with high resolution and theoretical plate numbers. An extension of the separation size range to 15 or 20 kbp can be obtained using low viscosity polymers (F. Xu et al. 2003) and with the addition bacterial cellulose fibrils to the low viscosity sieving medium (Tabuchi and Baba 2005). (Sun, Lin, and Barron 2011) could further extend the separation range to 40 kbp using polymer blends. They separated 13 bands in the size range of 1-40 kbp within 2 min.

Microchip gel electrophoresis (MGE) systems, where cross-linked gels like agarose are incorporated inside the microchannels, can also separate 1-20 kbp DNA. (Ghanim et al. 2013) used amperometric detection coupled with MGE in agarose to separate 1-20 kbp with a minimal RSL of 50 bp, however the separation took 37.5 min. (J.-H. Kim, Kang, and Kim 2005) used electrochemical detection with MGE to separate 1-10 kbp in 2.5 min. Most recently, (Gumuscu

et al. 2017) demonstrated that continuous separation can be performed using MGE. They fractionated 4 DNA bands of 1-10 kbp continuously within 2 min.

To overcome common limitations of MGE including Joule heating and limited reusability, artificial gels constructed using micro/nanofabrication techniques were developed. Nano-colloidal arrays (NCA), which are self-assembled closely-packed nanospheres were used to size 1-15 kbp bands using electro-hydrodynamic actuation in 1.7 min with high efficiency (Tabuchi et al. 2004). Using electrophoresis (Zeng and Harrison 2007) used NCA formed of 330-900 nm silica beads to continuously separate 2-27 kbp (Zeng, He, and Harrison 2008) as well as to fractionate two bands of 13 kbp and λ DNA (48.5 kbp) in 7 min. (Kuo et al. 2007) used NCA to form ordered nanoporous structure that resembles cross-linked gels to fractionate 1-10 kbp DNA in XX min.

Higher MW DNA up to 209 kbp could be separated using micro and nanopillar arrays (MPA/NPA). First, MPA enabled the separation of λ and T4 DNA (168.9 kbp) within 10 s using pulsed fields (Bakajin et al. 2001). (Lotien Richard Huang, Tegenfeldt, et al. 2002) also used alternating electric fields to continuously fractionate 4 bands in the range of 61-209 kbp in 15 s in a hexagonal array of 2 μ m diameter pillars called DNA prism. To facilitate the fabrication of pillar arrays, (Doyle et al. 2002) used self-assembled superparamagnetic nanoparticles that form 3D post arrays under a magnetic field form a coil. This technology could separate 3 bands of DNA in the ranges of 15-48.5 kbp and 48-145.5 kbp yet with low efficiency. Later, (Regtmeier et al. 2007) showed that MPA can be used for trapping long DNA using electrodeless dielectrophoresis. With the combination of electrophoresis and dielectrophoretic trapping, the separation of 7 and 14 kbp in addition to λ and T2 (164 kbp) was performed in 6 min.

NPA were widely used for the fast separation of few bands of DNA in the range of 1-166 kbp (Baba et al. 2003; Kaji et al. 2004; Chan, Lee, and Zohar 2006; Shi et al. 2007). (Yasui et al. 2015) showed that a non-equilibrium transport phenomenon inside NPA can yield fast separation of 3 bands of DNA of 1-48 kbp with very high efficiency (20×10^6 plates/m). (Rahong et al. 2014) fabricated a new structure of rigid 3D nanowire arrays to separate DNA of 1-166 kbp under DC electric field. The separation of 4 bands in this size range proved to be ultrafast in 13 sec (Kaji et al. 2004; Rahong et al. 2014). Most recently, high resolution separation of λ and T4 DNA was obtained in a nanorod sieving matrix fabricated using localized oblique angle deposition under constant electric field within 12 s (Cao et al. 2019). In general, MPA and NPA showed very fast separations of long DNA molecules, however only few bands could be fractionated with high RSL.

High MW DNA can also be separated using entropic trapping in slit-well motifs (SWM), which are alternating shallow slits and deep wells fabricated by photolithography. Long molecules stretch through the narrow slits and escape the traps faster than shorter molecules into the deep wells (J Han, Turner, and Craighead 1999). SWM were used to separate 8 bands of a 5-kbp DNA ladder with T2 and T7 DNA (37.9 kbp) and 4 bands of 24.5-97 kbp DNA in 15 to 40 min (J. Han and Craighead 2000; Jongyoon Han and Craighead 2002). A faster separation in 4 min of 6 bands in the range 3-21 kbp was obtained using a capillary well motif (CWM) with nano-capillaries of 750 nm diameters (Cao and Yobas 2014). Another entropic trapping device of

anisotropic nanofilter array (ANA) was developed to continuously separate 5 bands of 2-23 kbp in 1 min using orthogonal electric fields (Fu et al. 2007). Globally, entropic trapping in SWM feature even performances when compared to the other technologies (Table 1).

Obstacle arrays (OA) of different shapes and organization can be fabricated in microchannels to separate long DNA through several physical mechanisms. A Brownian Ratchet (BR) mechanism, where the DNA is separated based on differences in Brownian diffusion of different sizes in an array of obstacles, was used to separate λ and T2 DNA in 70-140 min (Lotien Richard Huang, Silberzan, et al. 2002; Lotien Richard Huang et al. 2003). Using this mechanism, the separation takes a long time since only low flow rates (or electric fields) can be used to allow for Brownian diffusion to separate the different species (Xuan and Lee 2014). Another mechanism that also relies on diffusion is size exclusion chromatography (SEC). In SEC, the array of obstacles forms narrow and wide gaps where smaller DNA molecules can pass through the narrow gaps while larger molecules continue their path in the wide gaps. SEC was used for the separation of 2, 5 and 10 kbp DNA in around 6 min (Baba et al. 2003). High flow rates can be used in OA with rows equally shifted with respect to one another. The separation mechanism in such an array was dubbed deterministic lateral displacement (DLD), since defined laminar flows that go through the OA control the path of molecules depending on their size. This technique was able to separate 61 and 158 kbp in 10 min (L. R. Huang et al. 2004). Separations in OA tend to be lengthy because they rely on molecular diffusion to achieve good performances.

Finally, through the adsorption of DNA on nano-patterned surfaces, 6 bands of 1-10 kbp could be separated with high resolution. This technique does not require the use of separation media and yields high theoretical plates, however, the fractionation of 1-8 kbp can take more than 30 min (Seo et al. 2004).

Compared to all the aforementioned methods, electro-hydrodynamic separation carried out in PermiNex chips compared favorably in terms of theoretical plates in the high MW limit, and featured the broadest analytical range, where 13 bands of 1-150 kbp were separated with a single round within less than 5 min (thick burgundy lines in Fig.7). Very noticeably, despite the use of hydrodynamics and the large breadth of the injection plug ($\sim 20 \mu\text{m}$, not shown), which tends to further increase band broadening due to Taylor dispersion, we achieved high theoretical plate numbers per m and low RSL of XX m^{-1} and XX bp , respectively, for molecules longer than 10^4 bp. This result is due to the confinement of molecules near the walls (as shown in Fig. 4), that restricts transverse fluctuations in a region where flow velocity variations are small.

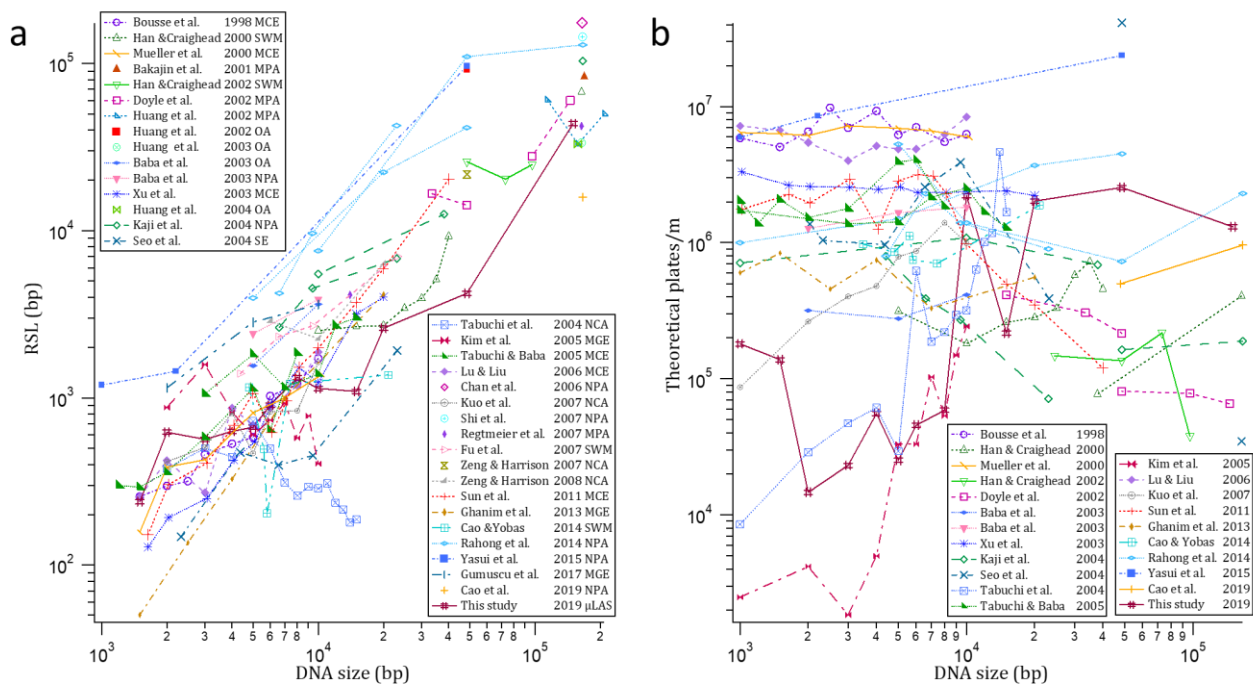


Figure 7: Comparison with state of the art microchip separation of long DNA. (a) Resolution length (RSL) for DNA molecules of 1-200 kbp obtained using different microchip separation techniques. The RSL defines the minimum size that can be resolved. (b) Theoretical plate numbers obtained using different microchip separation techniques. Our technology of electrohydrodynamic separation in viscoelastic polymers in glass/PermiNex/glass chips is comparable to the state of the art for long DNA separation.

Table 1: Comparison of microchip separation techniques for long DNA (1-200 kbp) in terms of size range, separation time, minimal RSL and theoretical plates/m.

Method	Method	(Kbp)	bands	Time (min)	RSL (Kbp)	(10 ⁶ plates/m)	Reference
MCE	PA	1 – 10	10	0.25	0.26	5.0 – 9.8	Bousse et al. 1998
	PA	1 – 10	7	1.4	0.16	5.9 – 7.2	Mueller et al. 2000
	Low viscosity HPMC	1 – 20	12	2.8	0.13	2.2 – 3.3	Xu et al. 2003
	cellulose fibrils	1 – 8	8	2.6	0.29	1.4 – 4	Tabuchi & Baba 2005
		1 – 15	7	2.4	1	1.3 – 1.7	
	LPA	1 – 10	9	6.2	0.26	4 – 8.4	Lu & Liu 2006
Polymer blend	1 – 40	13	2	0.15	0.1 – 3	Sun et al. 2011	
MGE	Agarose	1 – 20	6	37.5	0.05	0.3 – 0.6	Ghanim et al. 2013
	Agarose	1 – 10	10	2.5	0.4	0.0025 – 0.24	Kim et al. 2005
	Agarose	1 – 10	4	2	1	–	Gumuscu et al. 2017
NCA	PEGylated nanospheres /electro-hydrodynamic	1 – 15	15	1.7	0.18	0.008 – 4.6	Tabuchi et al. 2004
	Nanoporous SU-8 structure	1 – 10	8	10	0.4	0.2 – 1	Kuo et al. 2007
	Silica beads	13, λ	2	7	21.7	0.0058	Zeng & Harrison 2007
		6 – 20 2 – 27	4	–	2.8	–	Zeng & Harrison 2008
MPA	2 μ m-wide pillars/ Pulsed field	λ , T4	2	0.16	84	–	Bakajin et al. 2001
	2 μ m-wide pillars/ DNA prism	61 – 209	4	0.25	33	–	Huang et al. 2002
	1 μ m magnetic particles posts	15 – 48	3	15	14	0.2 – 0.4	Doyle et al. 2002
		48 – 145		30	28	0.06 – 0.08	
2 μ m posts/ Dielectrophoresis	7,14 λ , T2	2	6	4 42	–	Regtmeier et al. 2007	
NPA	150 nm pillars	2 – 10	3	1.25	2.4	1.27 – 1.8	Baba et al. 2003
	100-500 nm-wide pillars	4.4 – 23	4	11.3	2.6	0.07 – 0.8	Kaji et al. 2004
		1, 10, 38 λ , T4	3 2	2.8 0.38	5.5 103	0.7 – 1 0.16 – 0.19	
	300 nm pillars	21, T4	2	2	175	–	Chan et al. 2006
	200-300 nm wide pillars	λ , T4	2	2	14	0.002	Shi et al. 2007
	10-20 nm Nanowires (NWrA)	1 – 48	4	0.12	4	1 – 4.5	Rahong et al. 2014
		2 – 23	5	0.225	4	0.8 – 2.3	
		5 – 166	4	0.058	7.6	0.7 – 5.3	
500 nm wide pillars/ Nonequilibrium transport	1 – 48	3	1	1.2	6 – 20	Yasui et al. 2015	
Sub-100 nm nanorods	λ , T4	2	0.2	16	0.5 – 0.96	Cao et al. 2019	
SWM	75-100 nm slits & 1.5-3 μ m wells/ Entropic trapping	5 – 40	8	30	2.5	1 – 10	Han & Craighead 2000
		T7, T2	2	18.3	68	0.4	
	55 nm slits & 300 nm wells/ ANA	24 – 97	4	37	20	–	Han & Craighead 2002
		2 – 23	5	1	1.4	–	
750 nm capillaries & 13 μ m wells/ CWM	3.5 – 21	6	4	0.2	0.7 – 1.9	Cao & Yobas 2014	
OA	1.4 μ m obstacles/ BR	λ , T2	2	140	91	–	Huang et al. 2002
	1.4 μ m obstacles/ tilted BR	λ , T2	2	70	34	–	Huang et al. 2003
	2 μ m obstacles/SEC	2 – 10	3	5.8	1.6	0.27 – 0.4	Baba et al. 2003
	2.6 μ m obstacles/DLD	61, 158	2	10	33	–	Huang et al. 2004
SE	Ni patterned surface	2 – 23	6	33	0.15	1 – 3.9	Seo et al. 2004
μ LAS	PVP/ opposing electro- hydrodynamic	1 – 150	13	4.58	0.24	0.015 – 2.6	This study

CONCLUSION

The primary motivation of our work was the improvement of electro-hydrodynamic separation of high MW molecules using microchips. This objective is fulfilled as we show the separation of 14 DNA bands in the range of 0.5 to 150 kbp in less than 5 minutes with state-of-the-art RSL and theoretical plate number. This achievement has been reached through the implementation of a novel process for glass/adhesive/glass microchip fabrication, which offers several key advantages, namely (i) a very strong bonding strength, (ii) a low auto-fluorescence, and (iii) most importantly, homogeneous surface properties. A source of band broadening associated to differential EOF is indeed detected in heterogeneous microchip devices. Given that the inner surface of capillaries is homogeneous by virtue of design, it is tentative to suggest that the state-of-the-art format for high performance DNA separation remains the capillary despite years of research in Lab-on-Chip due to the hybrid format of most microchip devices (Ross, Johnson, and Locascio 2001).

Although surface coating is a well-worked out solution to reduce the EOF (Milanova et al. 2012; Kaneta et al. 2006; Ghosal 2004), it remains unclear whether its efficiency will be even on the surfaces of heterogeneous microchips. This remark is validated by the fact that the separation buffer of our experiments contains poly-vinylpyrrolidone, which is known to reduce the EOF (Milanova et al. 2012; Kaneta et al. 2006), and differential EOF is nevertheless detected in electrophoresis actuation. We therefore propose that our process for glass-adhesive-glass microchip fabrication could be useful to enhance the separation performances of virtually every separation technology based on electrophoretic, electro-hydrodynamic or hydrodynamic actuation.

ASSOCIATED CONTENT

Supporting Information

The supplementary material contains two figures. Supplementary Fig. S1 shows an electron micrograph of the section of PermiNex chips, and Supplementary Fig. S2 is a plot of the oxide breakdown voltage of Si-glass chips for different thicknesses of oxide.

AUTHOR INFORMATION

Corresponding Author

Correspondence should be sent to Aurélien BANCAUD (abancaud@laas.fr, +33 5 61 33 62 46)

The manuscript was written through contributions of all authors. All authors have given approval to the final version of the manuscript.

ACKNOWLEDGMENT

This work was partly supported by the LAAS-CNRS micro and nano-technologies platform, member of the French RENATECH network. B.C. PhD fellowship is supported by the “Ligue contre le cancer”. This project was partly supported by the project “Gene Extractor” from Région Midi-Pyrénées and by the ANR μ LAS (ANR-16-CE18-0028-01) and the ANR Biopulse (ANR-16-ASTR-0020).

REFERENCES

- Andreev, Victor P., Sergey G. Dubrovsky, and Yuri V. Stepanov. 1997a. “Mathematical Modeling of Capillary Electrophoresis in Rectangular Channels.” *Journal of Microcolumn Separations* 9 (6): 443–50. [https://doi.org/10.1002/\(SICI\)1520-667X\(1997\)9:6<443::AID-MCS1>3.0.CO;2-1](https://doi.org/10.1002/(SICI)1520-667X(1997)9:6<443::AID-MCS1>3.0.CO;2-1).
- Andreev, Victor P, Sergey G Dubrovsky, and Yuri V Stepanov. 1997b. “Mathematical Modeling of Capillary Electrophoresis in Rectangular Channels.” *Capillary Electrophoresis*, January, 443–50.
- Baba, M., T. Sano, N. Iguchi, K. Iida, T. Sakamoto, and H. Kawaura. 2003. “DNA Size Separation Using Artificially Nanostructured Matrix.” *Applied Physics Letters* 83 (7): 1468–70. <https://doi.org/10.1063/1.1602555>.
- Bakajin, Olgica, Thomas A. J. Duke, Jonas Tegenfeldt, Chia-Fu Chou, Shirley S. Chan, Robert H. Austin, and Edward C. Cox. 2001. “Separation of 100-Kilobase DNA Molecules in 10 Seconds.” *Analytical Chemistry* 73 (24): 6053–56. <https://doi.org/10.1021/ac015527o>.
- Bianchi, F., F. Wagner, P. Hoffmann, and H. H. Girault. 2001. “Electroosmotic Flow in Composite Microchannels and Implications in Microcapillary Electrophoresis Systems.” *Analytical Chemistry* 73 (4): 829–36. <https://doi.org/10.1021/ac0011181>.
- Biswas, K., and S. Kal. 2006. “Etch Characteristics of KOH, TMAH and Dual Doped TMAH for Bulk Micromachining of Silicon.” *Microelectronics Journal* 37 (6): 519–25. <https://doi.org/10.1016/j.mejo.2005.07.012>.
- Bousse, Luc, Bob Dubrow, and Kathi Ulfelder. 1998. “High-Performance DNA Separations in Microchip Electrophoresis Systems.” In *Micro Total Analysis Systems '98*, edited by D. Jed Harrison and Albert van den Berg, 271–75. Springer Netherlands.
- Cao, Zhen, and Levent Yobas. 2014. “Fast DNA Sieving through Submicrometer Cylindrical Glass Capillary Matrix.” *Analytical Chemistry* 86 (1): 737–43. <https://doi.org/10.1021/ac4031994>.
- Cao, Zhen, Yu Zhu, Yang Liu, Shurong Dong, Jiongdong Zhao, Ye Wang, Shu Yang, and Junxue Fu. 2019. “High-Resolution Separation of DNA/Proteins through Nanorod Sieving Matrix.” *Biosensors and Bioelectronics* 137 (July): 8–14. <https://doi.org/10.1016/j.bios.2019.04.033>.
- Chami, B., M. Socol, M. Manghi, and A. Bancaud. 2018. “Modeling of DNA Transport in Viscoelastic Electro-Hydrodynamic Flows for Enhanced Size Separation.” *Soft Matter* 14 (24): 5069–79. <https://doi.org/10.1039/C8SM00611C>.
- Chan, Yick Chuen, Yi-Kuen Lee, and Yitshak Zohar. 2006. “High-Throughput Design and Fabrication of an Integrated Microsystem with High Aspect-Ratio Sub-Micron Pillar Arrays for Free-Solution Micro Capillary Electrophoresis.” *Journal of Micromechanics and Microengineering* 16 (4): 699–707. <https://doi.org/10.1088/0960-1317/16/4/005>.
- Chen, Ping-Hei, Hsin-Yah Peng, Chia-Ming Hsieh, and Minking K Chyu. 2001. “The Characteristic Behavior of TMAH Water Solution for Anisotropic Etching on Both Silicon Substrate and SiO₂ Layer.” *Sensors and Actuators A: Physical* 93 (2): 132–37. [https://doi.org/10.1016/S0924-4247\(01\)00639-2](https://doi.org/10.1016/S0924-4247(01)00639-2).
- Deng, Wenhao. 2015. “Development of Glass-Glass Fusion Bonding Recipes for All-Glass Nanofluidic Devices.” Thesis, The Ohio State University. <https://kb.osu.edu/handle/1811/68597>.
- Dorfman, Kevin D. 2010. “DNA Electrophoresis in Microfabricated Devices.” *Reviews of Modern Physics* 82 (4): 2903–47. <https://doi.org/10.1103/RevModPhys.82.2903>.

- Doyle, P. S., Jerome Bibette, Aurelien Bancaud, and Jean-Louis Viovy. 2002. "Self-Assembled Magnetic Matrices for DNA Separation Chips." *Science* 295 (5563): 2237–2237. <https://doi.org/10.1126/science.1068420>.
- Fu, Jianping, Reto B. Schoch, Anna L. Stevens, Steven R. Tannenbaum, and Jongyoon Han. 2007. "A Patterned Anisotropic Nanofluidic Sieving Structure for Continuous-Flow Separation of DNA and Proteins." *Nature Nanotechnology* 2 (2): 121–28. <https://doi.org/10.1038/nnano.2006.206>.
- Ghanim, Motasem Hilmi, Nazalan Najimudin, Kamarulazizi Ibrahim, and Mohd Zaid Abdullah. 2013. "Low Electric Field DNA Separation and In-Channel Amperometric Detection by Microchip Capillary Electrophoresis." *IET Nanobiotechnology* 8 (2): 77–82. <https://doi.org/10.1049/iet-nbt.2012.0044>.
- Ghosal, Sandip. 2004. "Fluid Mechanics of Electroosmotic Flow and Its Effect on Band Broadening in Capillary Electrophoresis." *ELECTROPHORESIS* 25 (2): 214–28. <https://doi.org/10.1002/elps.200305745>.
- Giri, Basant. 2017. "2 - Fabrication of a Glass Microfluidic Device." In *Laboratory Methods in Microfluidics*, edited by Basant Giri, 9–20. Elsevier. <https://doi.org/10.1016/B978-0-12-813235-7.00002-7>.
- Gong, Xiuqing, Xin Yi, Kang Xiao, Shunbo Li, Rimantas Kodzius, Jianhua Qin, and Weijia Wen. 2010. "Wax-Bonding 3D Microfluidic Chips." *Lab on a Chip* 10 (19): 2622. <https://doi.org/10.1039/c004744a>.
- Gumuscu, Burcu, Johan G. Bomer, Hans L. de Boer, Albert van den Berg, and Jan C. T. Eijkel. 2017. "Exploiting Biased Reptation for Continuous Flow Preparative DNA Fractionation in a Versatile Microfluidic Platform." *Microsystems & Nanoengineering* 3 (May): 17001. <https://doi.org/10.1038/micronano.2017.1>.
- Han, J., and H. G. Craighead. 2000. "Separation of Long DNA Molecules in a Microfabricated Entropic Trap Array." *Science* 288 (5468): 1026–29. <https://doi.org/10.1126/science.288.5468.1026>.
- Han, J, S W Turner, and H G Craighead. 1999. "Entropic Trapping and Escape of Long DNA Molecules at Submicron Size Constriction." *PHYSICAL REVIEW LETTERS* 83 (8): 4.
- Han, Jongyoon, and Harold G. Craighead. 2002. "Characterization and Optimization of an Entropic Trap for DNA Separation." *Analytical Chemistry* 74 (2): 394–401. <https://doi.org/10.1021/ac0107002>.
- Herr, A. E., J. I. Molho, J. G. Santiago, M. G. Mungal, T. W. Kenny, and M. G. Garguilo. 2000. "Electroosmotic Capillary Flow with Nonuniform Zeta Potential." *Analytical Chemistry* 72 (5): 1053–57. <https://doi.org/10.1021/ac990489i>.
- Howlader, M.M.R., Satoru Suehara, and Tadatomo Suga. 2006. "Room Temperature Wafer Level Glass/Glass Bonding." *Sensors and Actuators A: Physical* 127 (1): 31–36. <https://doi.org/10.1016/j.sna.2005.11.003>.
- Huang, L. R., Edward C. Cox, R. H. Austin, and James C. Sturm. 2004. "Continuous Particle Separation Through Deterministic Lateral Displacement." *Science* 304 (5673): 987–90. <https://doi.org/10.1126/science.1094567>.
- Huang, Lotien Richard, Edward C. Cox, Robert H. Austin, and James C. Sturm. 2003. "Tilted Brownian Ratchet for DNA Analysis." *Analytical Chemistry* 75 (24): 6963–67. <https://doi.org/10.1021/ac0348524>.
- Huang, Lotien Richard, Pascal Silberzan, Jonas O. Tegenfeldt, Edward C. Cox, James C. Sturm, Robert H. Austin, and Harold Craighead. 2002. "Role of Molecular Size in Ratchet Fractionation." *Physical Review Letters* 89 (17): 178301. <https://doi.org/10.1103/PhysRevLett.89.178301>.
- Huang, Lotien Richard, Jonas O. Tegenfeldt, Jessica J. Kraeft, James C. Sturm, Robert H. Austin, and Edward C. Cox. 2002. "A DNA Prism for High-Speed Continuous Fractionation of Large DNA Molecules." *Nature Biotechnology* 20 (10): 1048–51. <https://doi.org/10.1038/nbt733>.
- Kaji, Noritada, Yojiro Tezuka, Yuzuru Takamura, Masanori Ueda, Takahiro Nishimoto, Hiroaki Nakanishi, Yasuhiro Horiike, and Yoshinobu Baba. 2004. "Separation of Long DNA Molecules by Quartz

- Nanopillar Chips under a Direct Current Electric Field." *Analytical Chemistry* 76 (1): 15–22. <https://doi.org/10.1021/ac030303m>.
- Kaneta, Takashi, Takeshi Ueda, Kazuki Hata, and Totaro Imasaka. 2006. "Suppression of Electroosmotic Flow and Its Application to Determination of Electrophoretic Mobilities in a Poly(Vinylpyrrolidone)-Coated Capillary." *Journal of Chromatography A* 1106 (1–2): 52–55. <https://doi.org/10.1016/j.chroma.2005.08.062>.
- Kim, Jonghyun, Il Kim, Yongwon Choi, and Kyung-Wook Paik. 2012. "Studies on the Polymer Adhesive Wafer Bonding Method Using Photo-Patternable Materials for MEMS Motion Sensors Applications." *IEEE Transactions on Components, Packaging and Manufacturing Technology* 2 (7): 1118–27. <https://doi.org/10.1109/TCPMT.2011.2178242>.
- Kim, Ju-Ho, C. J. Kang, and Yong-Sang Kim. 2005. "Development of a Microfabricated Disposable Microchip with a Capillary Electrophoresis and Integrated Three-Electrode Electrochemical Detection." *Biosensors and Bioelectronics* 20 (11): 2314–17. <https://doi.org/10.1016/j.bios.2005.01.015>.
- Kim, Min-Su, Seung Il Cho, Kook-Nyung Lee, and Yong-Kweon Kim. 2005. "Fabrication of Microchip Electrophoresis Devices and Effects of Channel Surface Properties on Separation Efficiency." *Sensors and Actuators B: Chemical* 107 (2): 818–24. <https://doi.org/10.1016/j.snb.2004.12.069>.
- Knechtel, Roy. 2012. "Glass Frit Wafer Bonding." In *Handbook of Wafer Bonding*, 1–17. John Wiley & Sons, Ltd. <https://doi.org/10.1002/9783527644223.ch1>.
- . 2015. "Chapter 31 - Glass Frit Bonding." In *Handbook of Silicon Based MEMS Materials and Technologies (Second Edition)*, edited by Markku Tilli, Teruaki Motooka, Veli-Matti Airaksinen, Sami Franssila, Mervi Paulasto-Kröckel, and Veikko Lindroos, 611–25. Micro and Nano Technologies. Boston: William Andrew Publishing. <https://doi.org/10.1016/B978-0-323-29965-7.00031-2>.
- Kubicki, Wojciech, Rafał Walczak, and Jan Dziuban. 2016. "Optical Properties and Real Application of New Photoimageable Bonding Adhesives." *Procedia Engineering* 168: 1402–5. <https://doi.org/10.1016/j.proeng.2016.11.394>.
- Kuo, Chiung-Wen, Jau-Ye Shiu, Kung Hwa Wei, and Peilin Chen. 2007. "Monolithic Integration of Well-Ordered Nanoporous Structures in the Microfluidic Channels for Bioseparation." *Journal of Chromatography A*, 21st International Symposium on Microscale Bioseparations, 1162 (2): 175–79. <https://doi.org/10.1016/j.chroma.2007.06.037>.
- Lu, Joann J., and Shaorong Liu. 2006. "A Robust Cross-Linked Polyacrylamide Coating for Microchip Electrophoresis of DsDNA Fragments." *ELECTROPHORESIS* 27 (19): 3764–71. <https://doi.org/10.1002/elps.200600201>.
- Mayer, Timo, Aleksei N Marianov, and David W Inglis. 2018. "Comparing Fusion Bonding Methods for Glass Substrates." *Materials Research Express* 5 (8): 085201. <https://doi.org/10.1088/2053-1591/aad166>.
- Milanova, Denitsa, Robert D. Chambers, Supreet S. Bahga, and Juan G. Santiago. 2012. "Effect of PVP on the Electroosmotic Mobility of Wet-Etched Glass Microchannels: Microfluidics and Miniaturization." *ELECTROPHORESIS* 33 (21): 3259–62. <https://doi.org/10.1002/elps.201200336>.
- Milon, Nicolas, Céline Chantry-Darmon, Carine Satge, Margaux-Alison Fustier, Stephane Cauet, Sandra Moreau, Caroline Callot, et al. 2019. "MLAS Technology for DNA Isolation Coupled to Cas9-Assisted Targeting for Sequencing and Assembly of a 30 Kb Region in Plant Genome." *Nucleic Acids Research* 47 (15): 8050–60. <https://doi.org/10.1093/nar/gkz632>.
- Mueller, Odilo, Karen Hahnenberger, Monika Dittmann, Herman Yee, Robert Dubrow, Rob Nagle, and Diane Ilsley. 2000. "A Microfluidic System for High-Speed Reproducible DNA Sizing and Quantitation." *ELECTROPHORESIS* 21 (1): 128–34. [https://doi.org/10.1002/\(SICI\)1522-2683\(20000101\)21:1<128::AID-ELPS128>3.0.CO;2-M](https://doi.org/10.1002/(SICI)1522-2683(20000101)21:1<128::AID-ELPS128>3.0.CO;2-M).

- Nathan A. Lacher, Kenneth E. Garrison, R. Scott Martin, and Susan M. Lunte. 2001. "Microchip Capillary Electrophoresis/ Electrochemistry." *Electrophoresis* 22: 2526–36.
- Niklaus, Frank. 2002. *Adhesive Wafer Bonding for Microelectronic and Microelectromechanical Systems*.
- Pfohl, Thomas, Frieder Mugele, Ralf Seemann, and Stephan Herminghaus. 2003. "Trends in Microfluidics with Complex Fluids." *ChemPhysChem* 4 (12): 1291–98.
<https://doi.org/10.1002/cphc.200300847>.
- Rahong, Sakon, Takao Yasui, Takeshi Yanagida, Kazuki Nagashima, Masaki Kanai, Annop Klamchuen, Gang Meng, et al. 2014. "Ultrafast and Wide Range Analysis of DNA Molecules Using Rigid Network Structure of Solid Nanowires." *Scientific Reports* 4 (June): 5252.
<https://doi.org/10.1038/srep05252>.
- Ranchon, Hubert, Rémi Malbec, Vincent Picot, Audrey Boutonnet, Pattamon Terrapanich, Pierre Joseph, Thierry Leïchlé, and Aurélien Bancaud. 2016. "DNA Separation and Enrichment Using Electro-Hydrodynamic Bidirectional Flows in Viscoelastic Liquids." *Lab on a Chip* 16 (7): 1243–53.
<https://doi.org/10.1039/C5LC01465D>.
- Ranchon, Hubert, Vincent Picot, and Aurélien Bancaud. 2015. "Metrology of Confined Flows Using Wide Field Nanoparticle Velocimetry." *Scientific Reports* 5 (1): 10128.
<https://doi.org/10.1038/srep10128>.
- Regtmeier, Jan, Thanh Tu Duong, Ralf Eichhorn, Dario Anselmetti, and Alexandra Ros. 2007. "Dielectrophoretic Manipulation of DNA: Separation and Polarizability." *Analytical Chemistry* 79 (10): 3925–32. <https://doi.org/10.1021/ac062431r>.
- Ross, David, Timothy J. Johnson, and Laurie E. Locascio. 2001. "Imaging of Electroosmotic Flow in Plastic Microchannels." *Analytical Chemistry* 73 (11): 2509–15. <https://doi.org/10.1021/ac001509f>.
- S G Serra, A Schneider, K Malecki, S E Huq, and W Brenner. 2007. "A Simple Bonding Process of SU-8 to Glass to Seal a Microfluidic Device." <https://doi.org/10.13140/2.1.2832.2082>.
- Schlautmann, S, G A J Besselink, G Radhakrishna Prabhu, and R B M Schasfoort. 2003. "Fabrication of a Microfluidic Chip by UV Bonding at Room Temperature for Integration of Temperature-Sensitive Layers." *Journal of Micromechanics and Microengineering* 13 (4): S81–84.
<https://doi.org/10.1088/0960-1317/13/4/313>.
- Seo, Young-Soo, H. Luo, V. A. Samuilov, M. H. Rafailovich, J. Sokolov, D. Gersappe, and B. Chu. 2004. "DNA Electrophoresis on Nanopatterned Surfaces." *Nano Letters* 4 (4): 659–64.
<https://doi.org/10.1021/nl0498435>.
- Shi, J, A P Fang, L Malaquin, A Pépin, D Decanini, J L Viovy, and Y Chen. 2007. "Highly Parallel Mix-and-Match Fabrication of Nanopillar Arrays Integrated in Microfluidic Channels for Long DNA Molecule Separation." *Appl. Phys. Lett.*, 4.
- Stjernström, Mårten, and Johan Roeraade. 1998. "Method for Fabrication of Microfluidic Systems in Glass." *Journal of Micromechanics and Microengineering* 8 (1): 33–38.
<https://doi.org/10.1088/0960-1317/8/1/006>.
- Sun, Mingyun, Jennifer S. Lin, and Annelise E. Barron. 2011. "Ultrafast, Efficient Separations of Large-Sized DsDNA in a Blended Polymer Matrix by Microfluidic Chip Electrophoresis: A Design of Experiments Approach." *ELECTROPHORESIS* 32 (22): 3233–40.
<https://doi.org/10.1002/elps.201100260>.
- Suttijalern, Kamonwan, Jirawat Prabket, and Surasak Niemcharoen. 2018. "Study of UMSM Photodetectors Fabrication Technique by Silicic Acid Added in TMAH Solution." *Hong Kong*, 4.
- Tabuchi, Mari, and Yoshinobu Baba. 2005. "Design for DNA Separation Medium Using Bacterial Cellulose Fibrils." *Analytical Chemistry* 77 (21): 7090–93. <https://doi.org/10.1021/ac0511389>.
- Tabuchi, Mari, Masanori Ueda, Noritada Kaji, Yuichi Yamasaki, Yukio Nagasaki, Kenichi Yoshikawa, Kazunori Kataoka, and Yoshinobu Baba. 2004. "Nanospheres for DNA Separation Chips." *Nature Biotechnology* 22 (3): 337–40. <https://doi.org/10.1038/nbt939>.

- Viovy, Jean-Louis. 2000. "Electrophoresis of DNA and Other Polyelectrolytes: Physical Mechanisms." *Reviews of Modern Physics* 72 (3): 813–72. <https://doi.org/10.1103/RevModPhys.72.813>.
- Wang, Xiayan, Lei Liu, Qiaosheng Pu, Zaifang Zhu, Guangsheng Guo, Hui Zhong, and Shaorong Liu. 2012. "Pressure-Induced Transport of DNA Confined in Narrow Capillary Channels." *Journal of the American Chemical Society* 134 (17): 7400–7405. <https://doi.org/10.1021/ja302621v>.
- Xu, Feng, Mohammad Jabasini, Shaoqian Liu, and Yoshinobu Baba. 2003. "Reduced Viscosity Polymer Matrices for Microchip Electrophoresis of Double-Stranded DNA." *The Analyst* 128 (6): 589. <https://doi.org/10.1039/b300247k>.
- Xu, Yan, Chenxi Wang, Yiyang Dong, Lixiao Li, Kihoon Jang, Kazuma Mawatari, Tadatomo Suga, and Takehiko Kitamori. 2012. "Low-Temperature Direct Bonding of Glass Nanofluidic Chips Using a Two-Step Plasma Surface Activation Process." *Analytical and Bioanalytical Chemistry* 402 (3): 1011–18. <https://doi.org/10.1007/s00216-011-5574-2>.
- Xuan, Jie, and Milton L. Lee. 2014. "Size Separation of Biomolecules and Bioparticles Using Micro/Nanofabricated Structures." *Anal. Methods* 6 (1): 27–37. <https://doi.org/10.1039/C3AY41364K>.
- Yasui, Takao, Noritada Kaji, Ryo Ogawa, Shingi Hashioka, Manabu Tokeshi, Yasuhiro Horiike, and Yoshinobu Baba. 2015. "Arrangement of a Nanostructure Array To Control Equilibrium and Nonequilibrium Transports of Macromolecules." *Nano Letters* 15 (5): 3445–51. <https://doi.org/10.1021/acs.nanolett.5b00783>.
- Zeng, Yong, and D. Jed Harrison. 2007. "Self-Assembled Colloidal Arrays as Three-Dimensional Nanofluidic Sieves for Separation of Biomolecules on Microchips." *Analytical Chemistry* 79 (6): 2289–95. <https://doi.org/10.1021/ac061931h>.
- Zeng, Yong, Mei He, and D Jed Harrison. 2008. "Microfluidic Self-Patterning of Large-Scale Crystalline Nanoarrays for High-Throughput Continuous DNA Fractionation*." *Angew. Chem.*, 4.
- Zheng, Jinjian, and Edward S. Yeung. 2002. "Anomalous Radial Migration of Single DNA Molecules in Capillary Electrophoresis." *Analytical Chemistry* 74 (17): 4536–47. <https://doi.org/10.1021/ac0257344>.